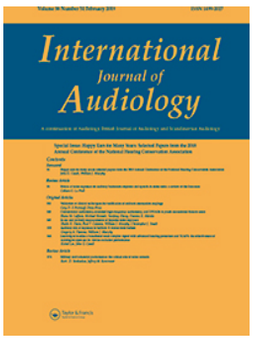

International Journal of Audiology

ISSN: 1499-2027 (Print) 1708-8186 (Online) Journal homepage: https://www.tandfonline.com/loi/iija20

Auditory risk of exposure to ballistic N-waves from bullets

Gregory A. Flamme & William J. Murphy

To cite this article: Gregory A. Flamme & William J. Murphy (2019) Auditory risk of exposure to ballistic N-waves from bullets, International Journal of Audiology, 58:sup1, S58-S64, DOI: 10.1080/14992027.2018.1534009

To link to this article: https://doi.org/10.1080/14992027.2018.1534009

INTERNATIONAL JOURNAL OF AUDIOLOGY
2019, VOL. 58, NO. S1, S58–S64
https://doi.org/10.1080/14992027.2018.1534009

The British Society of Audiology
The International Society of Audiology
NAS NORDIC AUDIOLOGICAL SOCIETY
Taylor & Francis
Taylor & Francis Group

ORIGINAL ARTICLE

Auditory risk of exposure to ballistic N-waves from bullets

Gregory A. Flamme[a] and William J. Murphy[b]

[a]Stephenson and Stephenson Research and Consulting, Forest Grove, OR, USA; [b]Hearing Loss Prevention Team, Engineering and Physical Hazards Branch, Division of Applied Research and Technology, National Institute for Occupational Safety and Health, Cincinnati, OH, USA

ABSTRACT

Objective: Assessment of the auditory risk associated with sound from ballistic N-waves produced by a rifle bullet.

Design: Acoustical recordings of ballistic N-waves passing through a microphone array at 6.4 metres down range were analysed to determine (a) the trajectory of the bullet, (b) the distance between the trajectory and each microphone (less than 1.3 m), and (c) the numbers of permissible exposures according to both damage-risk criteria for impulsive noise in the current U.S. military standard (MIL-STD-1474E).

Study Sample: The gun was an AR-15 style semiautomatic rifle configured to fire a 0.50 calibre Beowulf® cartridge. Four sample shots were recorded for each of four microphone spacing conditions and five kinds of ammunition (80 shots in total).

Results: The ballistic N-waves recorded in this study would constitute a significant auditory risk to unprotected listeners at all distances sampled. The numbers of permissible exposures decreased as the distance to the bullet trajectory decreased, decreased with increased bullet length, and departed from linear increases as the bullet velocity increased.

Conclusions: Unprotected exposure to a ballistic N-wave from a supersonic 0.50 calibre bullet presents a significant risk to hearing at distances of 6.4 metres down range and through trajectories within 1.2 metres of an ear.

ARTICLE HISTORY
Received 30 May 2018
Accepted 28 September 2018

KEYWORDS
hearing conservation; noise; impulses; risk; noise-induced hearing loss

Background

Routine exposure to the sound of a passing bullet is unlikely. However, some occupational groups might experience this noise exposure. Military training and operations can include multiple warfighters firing weapons at multiple targets, and those targets could require a trajectory passing near members of the fire team. Similar circumstances can occur in law enforcement training and operations. Non-occupational exposures are less common but include team tactical shooting done during leisure time and exposures incidental to gun violence.

For a bullet travelling faster than the speed of sound, an N-shaped ballistic shock wave (N-wave) will precede the muzzle blast if the listener is located in front of the weapon (Figure 1). Unlike stationary sound sources, which radiate sound spherically, the N-wave is a wake that expands conically from the path of a supersonic bullet. The angle of the cone surface relative to the trajectory is inversely proportional to bullet speed, v, and approaches 90 degrees as the projectile reaches the speed of sound, c. The spherical expansion of the muzzle blast is centred just in front of the muzzle.

The N-wave is characterised by a sharp positive pressure wavefront that decays linearly to a rarefaction before an abrupt return to ambient pressure. The theory describing the formation, amplitude and duration of the N-wave has been developed by Landau (1942) and DuMond et al. (1946). DuMond et al. (1946) investigated the dependence of the amplitude and period of the N-wave with the miss distance (nearest approach) of the bullet's trajectory and the microphone. Whitham (1974) provided the formulation of the maximum pressure in the acoustic far field as

$$p_{\mathrm{Max}} = \frac{0.53 p_0 (M^2-1)^{1/8}}{b^{3/4}} \frac{d}{l^{1/4}}, \quad (1)$$

where p_0 is the ambient pressure, $M = v/c$ is the Mach number, b is the miss distance, d is the bullet diameter, and l is the length of the bullet. The waveform is produced at every point along the trajectory as long as the projectile is moving faster than the speed of sound. The amplitude of the N-wave increases monotonically with bullet velocity (v) and projectile diameter. The amplitude decreases with projectile length and miss distance from the point at which it was produced.

Most assessments of auditory risks of firearms have focussed on locations behind the muzzle and well away from the bullet trajectory. The few studies evaluating the acoustic characteristics of N-waves produced by small firearms (e.g. DuMond et al., 1946; Stoughton, 1997; Varnier and Sourgen, 2014) have been conducted at miss distances of 2 m or greater.

The literature provides reasonable indications that that theory underestimates observed peak levels by as few as 2 dB, shown with 5.56 mm and 7.62 mm projectiles (Stoughton, 1997) or as much as 6 dB with 12.7 and 40 mm projectiles (Varnier & Sourgen, 2014). Stoughton (1997) proposed that deviations from the predictions involve sound channel focussing, which could be related to differential refraction from temperature gradients between the ground and the bullet trajectory. It is not clear whether the projectile dimensions or the velocity contribute

CONTACT Gregory A. Flamme gflamme@sasrac.com Stephenson and Stephenson Research and Consulting 2264 Heather Way, Forest Grove, OR 97116, USA

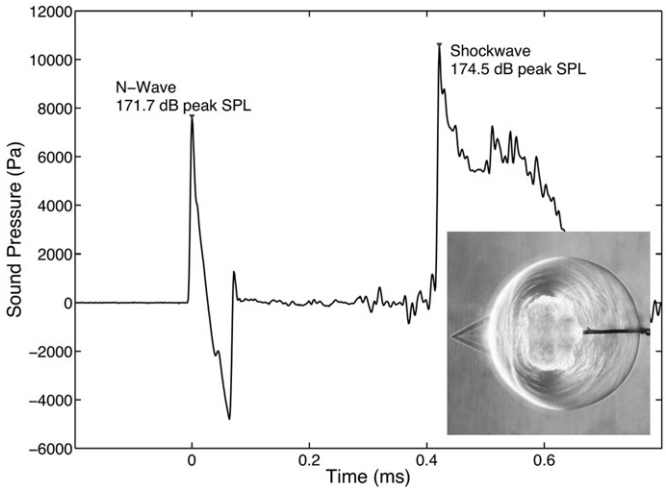

Figure 1. The ballistic shock wave and muzzle blast from a bullet that is travelling at supersonic velocity. The bullet travels faster than the spherical expansion of the muzzle blast to produce a cone shaped shock wave as illustrated in the inset Schleiren photograph. Inset image used with permission from Settles (2001).

most to the difference, but it is plausible that larger deviations will be observed with larger projectile diameters.

Fedele et al. (2018) considered the contributions of auditory risk from two portions (N-wave and muzzle blast) of the waveform produced by 5.56 mm (M4 rifle) and 7.62 mm (M110) rifle. Their study placed two arrays of four microphones at 5 and 10 m and 6, 12, 18 and 24 degrees from the muzzle and direction of fire. Fedele et al. (2018) did not compare their waveforms to the theoretical predictions (Equations 1 and 2). The choice of distance from the muzzle and the angles facilitates a comparison of the 5 m, 12° with 10 m, 6° and a comparison of 5 m, 24° with 10 m, 12° because the miss distances are within 0.6 and 4.5 cm, respectively. The peak levels for both weapons and both microphone comparison positions were identical. Fedele et al. (2018) reported the Auditory Risk Units (ARUs) and 8-h A-weighted equivalent energy, L_{Aeq8}, for these positions. The L_{Aeq8} values agreed within a few tenths of a decibel and the ARUs for three of the four comparisons agreed within 10%. The fourth comparison point was different by about 50%. However, the ARU metric is linear whereas the L_{Aeq8} metric is logarithmic.

The distance between the measurement location and the nearest point along the bullet trajectory (i.e. the miss distance) is a crucial aspect of assessing auditory hazard as a function of distance. The potential hazard associated with ballistic N-wave exposure is expected to grow rapidly as the miss distance declines, but most empirical studies of ballistic N-wave characteristics have been conducted at greater miss distances than can best inform evaluations of auditory risk. Physical targets in the vicinity of the microphones are undesirable because they would produce unwanted reflections. The current study develops a method for determining the miss distance, assesses the auditory risk associated with ballistic N-wave exposure, and examines the results obtained with one gun. Specifically, this study addressed the question of whether the ballistic N-wave produced by the nearby passing of a single supersonic projectile from a large-calibre civilian rifle exceeds the auditory damage risk criteria for unprotected noise exposures.

This work was motivated by an event involving a law enforcement officer who was fired upon by a shooter armed with a 0.50 calibre Beowulf® AR-15 style rifle. In order to assess the potential risk associated with this unprotected exposure, the authors worked with an Indiana State Police officer who provided and fired a personally-owned 0.50 calibre Beowulf® rifle.

Method

The assessment of auditory risk as a function of miss distance depends on an accurate determination of the trajectory followed by the bullet. This determination is based on observed time differences across an array of microphones at known locations. The coordinate system for this study has the y-axis along the length of the firing range; the x-axis is right and left of the muzzle and the z-axis is the vertical distance above the ground (see Figure 2 left panel). Four sets of microphone positions, spanning a horizontal distance of 1.35 m, were used in this study (Table 1). The intended bullet trajectory was along the y-axis, 0.15 m from microphones 3 and 4, at an elevation of 1.16 m.

The relative times of arrival for the N-waves at the microphones were analysed to determine the speed of the bullet; the intersection of the bullet's trajectory with the plane formed by microphones 1, 2 and 3; and the intersection of the bullet's trajectory with the plane formed by microphones 1, 2 and 4 (Figure 2). The bullet speed was estimated from the difference in the time of arrival (DTOA) of the N-wave at microphones 3 and 4,

$$v = \frac{|\boldsymbol{r}_3 - \boldsymbol{r}_4|}{\Delta t_{34}} = \frac{0.95}{\Delta t_{34}} \text{ m/s}, \tag{2}$$

where $\Delta t_{34} = t_4 - t_3$, the arrival times at microphones 3 and 4. For a given Mach number, $M = v/c$, the interior half angle, $\pi/2 - \theta$, of the cone of the N-wave is illustrated in Figure 3 as it propagates away from the trajectory (Korman and Sarkady, 2013). The angle, θ, is defined

$$\theta = \cos^{-1}\left(\frac{c}{v}\right). \tag{3}$$

The change in the speed of the bullet due to air friction is negligible as it passes between the two points where the N-wave separates and propagates to microphones 3 and 4. Effects on the trajectory due to gravity were considered trivial because they are small relative to the 12.7 mm diameter of the 0.50 calibre bullet. Over the length of the range (muzzle to microphones), 6.40 and 7.35 m, gravity effects produce a drop between 0.4 and 1.3 mm. Over the distance between microphones 3 and 4, the drop due to gravity will be of the order of 0.025 mm. The average temperature was 22°C during data collection. The change in temperature during the data collection period was 1.8°C. The speed of sound used in the calculations was $c = 345$ m/s. Changes in the speed of sound that might have arisen from changes in the ambient temperature or the shock wave's outward radial propagation speed had negligible effects on the estimates of miss distance.

The geometry used to solve for the time of arrival (TOA) of the N-wave is shown in Figure 3. The muzzle location was nominally located at $\boldsymbol{r}_0 = [0,\ 0, z_{\text{bullet}}]$, where z_{bullet} was 1.40 m. Because the range may have had a slight elevation change from the muzzle to the microphone array, a grid of several possible origin coordinates was searched: $(-0.25 \le x \le 0.25)$ and $(1.25 \le z \le 1.75)$. The y coordinate corresponds to the downrange position of the microphones. In Figure 3, the microphone is located at $\boldsymbol{r}_i$. Microphones 1, 2 and 3 and microphones 1, 2 and 4 formed two planes through which the bullet passed. By determining the DTOA for the microphone pairs in the respective planes, a unique solution was found for the trajectory.

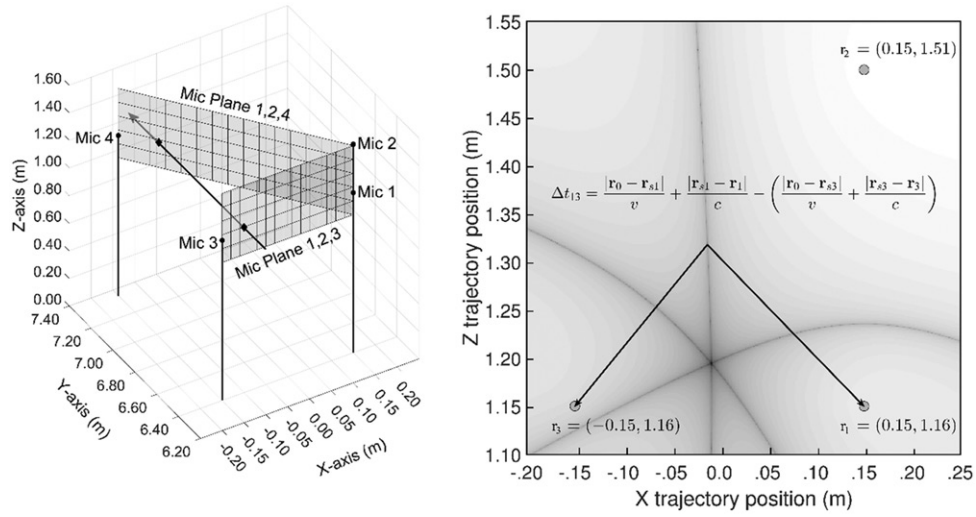

Figure 2. Microphone positions, microphone planes and hypothetical bullet trajectory. Four sets of microphone positions were used with microphones 1 and 2 at $x = 0.15$, 0.30, 0.60 and 1.2 metres. The planes formed by microphones 1, 2 and 3 and by microphones 1, 2 and 4 are depicted. The grid used to estimate the trajectory had a spacing of 1.25 cm in the x and z directions, approximately half the diameter of the 0.50 calibre bullet.

Table 1. The three-dimensional coordinates ([x, y, z]) of the microphones.

	Position 1	Position 2	Position 3	Position 4
Mic 1	[0.15, 6.40, 1.16]	[0.30, 6.40, 1.16]	[0.60, 6.40, 1.16]	[1.20, 6.40, 1.16]
Mic 2	[0.15, 6.40, 1.51]	[0.30, 6.40, 1.51]	[0.60, 6.40, 1.51]	[1.20, 6.40, 1.51]
Mic 3	[−0.15, 6.40, 1.16]	[−0.15, 6.40, 1.16]	[−0.15, 6.40, 1.16]	[−0.15, 6.40, 1.16]
Mic 4	[−0.15, 7.35, 1.16]	[−0.15, 7.35, 1.16]	[−0.15, 7.35, 1.16]	[−0.15, 7.35, 1.16]

The muzzle of the rifle was nominally located at [0.00, 0.00, 1.40] metres. The y-axis is the distance down range, the x-axis is right and left of the muzzle and the z-axis is the vertical distance above the ground.

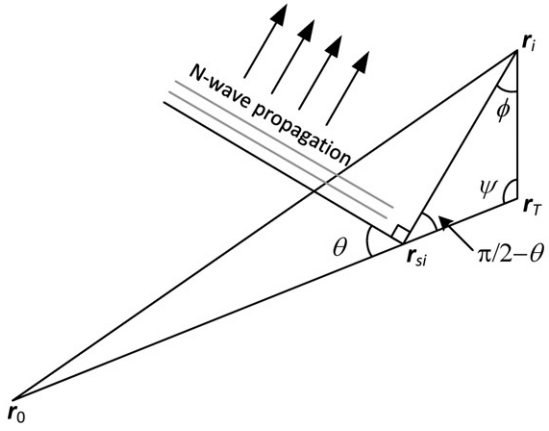

Figure 3. Definition of angles for the N-wave from a plan perspective. The muzzle of the firearm is located at $r_0 = [0,\ 0, z_{\text{bullet}}]$ and the measurement microphone is positioned at $r_i = [x_i, y_i, z_i]$. The bullet intersects the measurement plane at $r_T = [x_T, y_T, z_T]$. The angle between the measurement microphone, r_i, the muzzle, r_0, and the trajectory is, ψ_i. The wavefront from the N-wave originates at r_{si} and propagates to r_i at the speed of sound to the microphone position. The wavefront moves along an angle, θ, relative to the trajectory.

Because all of the shots were fired at the same target from a fixed location, possible trajectory intersections, r_T were considered from $-0.25 \le x \le 0.25$ and $0.90 \le z \le 1.40$ with a 5 mm grid spacing. The angle formed by $r_0 - r_T$ and $r_i - r_T$ was determined

$$\psi_i = \cos^{-1}\left(\frac{(r_0 - r_T)\cdot(r_i - r_T)}{|r_0 - r_T||r_i - r_T|}\right). \quad (4)$$

The numerator is the dot product between the vectors defining the directions between the origin, r_0, to the point of the trajectory's intersection with the plane, r_T, and the microphone at position i, r_i, to r_T. The magnitudes of those difference vectors are given in the denominator. The N-wave separates from the trajectory at r_{si} and propagates at the speed of sound to the microphone at r_i. The angle formed by $r_T - r_i$ and $r_{si} - r_i$ is $\varphi_i = \pi - \theta - \psi_i$. The law of sines is used to find the distance from the separation point to the i^{th} microphone,

$$|r_i - r_{si}| = \sin(\psi_i)\frac{|r_i - r_T|}{\sin(\theta)}. \quad (5)$$

Similarly, the distance from the muzzle to the separation point is

$$|r_0 - r_{si}| = |r_0 - r_T| - |r_{si} - r_T| = |r_0 - r_T| - \sin(\varphi_i)\frac{|r_i - r_T|}{\sin(\theta)}. \quad (6)$$

The TOA from any muzzle location to any microphone position is the summation of the time for the bullet to travel from the gun to the separation point, plus the time for the N-wave to travel from the separation point to the microphone position,

$$t_i = \frac{|r_0 - r_{si}|}{v} + \frac{|r_{si} - r_i|}{c}. \quad (7)$$

Then the DTOA for two microphones at positions r_i and r_j, is

$$\Delta t_{ij} = \frac{|r_0 - r_{si}|}{v} + \frac{|r_{si} - r_i|}{c} - \left(\frac{|r_0 - r_{sj}|}{v} + \frac{|r_{sj} - r_j|}{c}\right), \quad (8)$$

where i and j are the microphone subscripts. Note that the separation points of the N-wave along the trajectory will only coincide if the trajectory is an equal distance from each microphone

Table 2. Ammunition characteristics.

Label	Nominal muzzle velocity, m/s (feet/s)	Observed velocity*, m/s	Observed Mach number*	Interior half-angle of Mach cone, degrees	Bullet length, cm
200g PolyCase® inceptor	762 (2500)	694	2.01	29.8	2.2
335g Rainer FMJ	573 (1880)	535	1.55	40.2	1.9
350g Millenium brass spitzer	506 (1661)	475	1.38	46.6	2.9
350g Hornady® XTP®	533 (1750)	490	1.42	44.8	2.1
400g FP Hawk	555 (1820)	486	1.41	45.2	2.3

*Observed at the microphone array.

(i.e. on a line bisecting the two microphones). Subtracting the measured DTOA from the calculated DTOA defines a surface computed for the possible range of trajectory locations. For a given Δt_{ij}, a hyperbola describes the possible trajectory positions that would satisfy the measured Δt_{ij} for the arrival of the N-wave at the microphone pair (see Figure 2 right panel). Because the three pairs of microphones were co-planar, the intersection of the hyperbolae within the plane specifies where the bullet passed. The two intersection points, $\boldsymbol{r}_{\mathrm{T}\ 1,2,3}$ and $\boldsymbol{r}_{\mathrm{T}\ 1,2,4}$, define the trajectory used to estimate the miss distance to any microphone, $\boldsymbol{r}_i$.

Following a similar derivation of the DTOA, the angle, ξ_i, between the trajectory vector and the microphone location can be found

$$\xi_i = \cos^{-1}\left(\frac{(\boldsymbol{r}_{\mathrm{T}\ 1,2,3}-\boldsymbol{r}_{\mathrm{T}\ 1,2,4})\cdot(\boldsymbol{r}_i-\boldsymbol{r}_{\mathrm{T}\ 1,2,4})}{|\boldsymbol{r}_{\mathrm{T}\ 1,2,3}-\boldsymbol{r}_{\mathrm{T}\ 1,2,4}||\boldsymbol{r}_i-\boldsymbol{r}_{\mathrm{T}\ 1,2,4}|}\right). \quad (9)$$

The magnitude of the miss distance (i.e., the distance between the microphone and the nearest point along the bullet trajectory) is then

$$b = |\boldsymbol{r}_{\mathrm{i}}-\boldsymbol{r}_{\mathrm{T}\ 1,2,4}|\sin(\xi_i). \quad (10)$$

Rifle and ammunition

The firearm used in this study was a semi-automatic rifle (AR-15 style) with a 42 cm (16.5 inch) barrel chambered for a 0.50 Beowulf® cartridge (Alexander Arms Inc., Blacksburg, VA). The advantages of this weapon for this purpose are that it has: one of the largest projectile diameters for small arms; a variety of available ammunition velocities and dimensions; and only one manufacturer produces 0.50 Beowulf® ammunition, which maximises consistency and generalisability.

The ammunition selected for this study spanned the range of available muzzle velocities and bullet dimensions for this rifle. Five of the seven available types of ammunition for the gun were used in this study (Table 2).

Instrumentation

Recordings were obtained using four G.R.A.S. Type 40DP 1/8-inch pressure-calibrated microphones (1 mV/Pa nominal sensitivity, 178 dB max. input level), which were oriented perpendicular to the bullet trajectory through the array. Three G.R.A.S. preamplifiers (Type 26AC or Type 26TC) having a 20 V/μs slew rate were used with the microphones on the front plane (microphones 1 through 3). A Brüel & Kjaer Type 2670 preamplifier (2 V/μs slew rate) was used with the rear microphone (microphone 4). All microphones were externally polarised (200 V) using G.R.A.S. Type 12AA power supplies. Signals were recorded digitally at 200 kHz sampling rate with 24-bit resolution and a ± 42 volt dynamic range using a National Instruments PXI-4462 dynamic signal analyser module mounted in a PXIe-1082 chassis and controlled using a personal computer running custom LabVIEW® (Austin, TX) functions. Field calibration of microphones was conducted before and after impulse measurements using a G.R.A.S. Type 42AP pistonphone.

Procedure

Recordings were made on an otherwise unoccupied private firing range. The gun was mounted in a stand and the microphone array was positioned on a grass-covered level surface 6.4 metres down range from the muzzle. The analysis only considered the N-wave as it arrived at the microphones. Any other reflections from the ground, gun stand, researchers etc. were excluded by a time-window. Sounds from four rounds of each type of ammunition were recorded for each separation distance of the front three microphones (1, 2 and 3). The position of the gun in the stand was monitored and adjusted as necessary between measurements.

Data analyses

Following data acquisition, data management, review, and processing tasks were conducted using custom MATLAB® functions (Mathworks, Inc., Natick, MA). Miss distance determinations were made using the theory described above.

Risk estimates were obtained using both damage-risk metrics included in MIL-STD-1474E (2015). One of these metrics, $L_{IAeq8hr}$, is based on the integrated A-weighted energy in the signal. The calculation of $L_{IAeq8hr}$ was done following the guidelines of MIL-STD-1474E (United States Department of Defense, 2015). Briefly, these calculations involved integrating the energy over the N-wave duration after applying an A-weighting filter to the signal. This metric adjusts risk estimates based on the pressure-wave duration of some signals, but the pressure-wave durations of these signals were below the lower-limit of those adjustments and therefore had no effect. Equivalent continuous levels for each N-wave were then transformed into 8-hour equivalent values.

The other metric, the Auditory Hazard Assessment Algorithm for Humans (AHAAH) version 2.1, is based on estimates of summed upward basilar membrane displacements after the signal has been passed through a model intended to emulate the average human ear. The N-wave peaks were identified in MATLAB and a 5 ms pretrigger interval was used to provide the start of the waveform analysed by the AHAAH model. The duration of the windowed waveform including the N-wave was 82 ms. This time-window excluded the muzzle blast because the exposure of interest was just the ballistic shock wave. The beginning and end of the waveform were tapered with a 1 ms raised cosine function (half of a 2 ms Hann window) to remove any non-zero transients at the start of the analysed segment that could affect the result

artifactually. The taper function did not affect the amplitude of the wave anywhere else. The waveforms were written to an ASCII .AHA file to facilitate processing with the AHAAH software. Although these methods are very strongly correlated with one another, the AHAAH model tends to assign greater hazard to short-duration impulses from small arms (Flamme et al., 2009). The temporal and spectral characteristics of the N-wave could produce a different relationship between the metrics.

Determination of maximum permissible exposures (MPE) based on the $L_{IAeq8hr}$ metric was conducted using custom MATLAB® functions (Mathworks, Inc., Natick, MA). The numbers of maximum permissible exposures were determined by

$$MPE = 10^{\frac{(85 - L_{IAeq8hr})}{10}}. \quad (11)$$

Exposure limits based on the AHAAH metric were based on unwarned auditory risk unit (ARU) calculations returned by stand-alone software operating in a Windows software environment and converted into MPE by dividing 500 by the observed ARU value (MIL-STD-1474E). All MPE estimates were made assuming that an exposed listener had no hearing protection.

Risk estimates were produced only for the signals from the two microphones most distant from the bullet trajectory. The signals from the other two microphones were sufficient for TOA-based analyses, but the N-waves reaching the microphones 3 and 4 (see Figure 2) frequently had amplitudes greater than the specified microphone limits or had signal rise times that were at or above the specified maximum slew rate of the preamplifier.

Factors related to risk estimates were identified using a multilevel linear regression model wherein the numbers of permissible exposures were predicted by miss distance, measured bullet velocity, and bullet length. The multilevel model accounted for the presence of multiple observations (i.e. recordings at each microphone) each time the gun was fired. Although the residual errors from these models approximated a normal distribution, robust standard error estimates (Huber, 1967) were used. Stata® v. 15 (StataCorp LLC, College Station, TX) software was used for all inferential analyses.

Results

The bullets travelled through a space less than 0.2 m wide and 0.35 m tall. In Figure 4, the intersection of the bullet trajectories with the microphone planes are shown with x and + symbols. The x symbols represent the intersection of the trajectories with the microphone plane 1, 2, 3 and the + symbols represent the intersections with microphone plane 1, 2, 4 indicated that the bullets passed microphones 3 and 4 at distances of 15 cm or less, and that, following repositioning of the gun in the stand, some bullets passed within a few centimetres of that microphone.

In the upper panel of Figure 5, observed peak levels (open squares) and predicted peak levels (filled circles) are shown as a function of the miss distance. The predicted levels were calculated using Equation 1 indicated that expectations derived for far-field conditions underestimated the peak levels observed in this study. In the lower panel of Figure 5, the mean difference was approximately 4 dB (SD: 1 dB) and did not differ substantially as a function of miss distance.

Estimates of auditory risk were calculated using the $L_{IAeq8hr}$ and unwarned ARU metrics and converted into MPE. Non-integer MPEs were retained for analyses but were converted to the next lower integer value for reporting due to the impossibility of exposure to only part of an impulsive sound. For example, two permissible exposures would be reported for an N-wave yielding an 81 dB $L_{IAeq8hr}$ and three exposures would be permitted for an N-wave yielding 150 ARUs.

In Figure 6, the MPE values using the $L_{IAeq8hr}$ metric increased monotonically as a function of miss distance. Only one

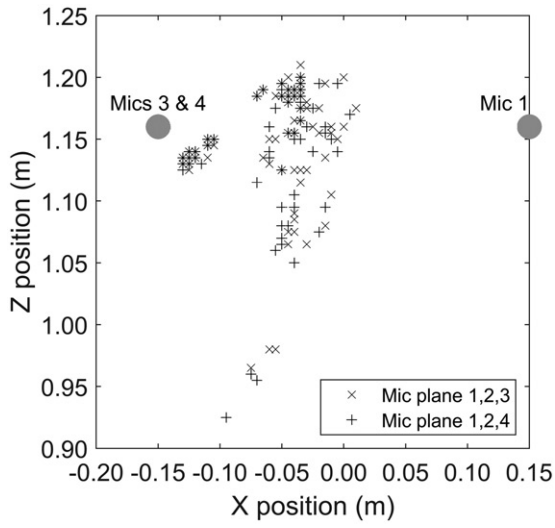

Figure 4. The estimated positions of the intersection of the bullet trajectories for the planes formed by microphones 1, 2 and 3, and microphones 1, 2 and 4. Microphone plane 1, 2 and 3 was nominally perpendicular to the bullet trajectory while the microphone plane 1, 2 and 4 was at an angle that changed as microphones 1 and 2 were moved further away. The *x* coordinate was the distance from the line formed by microphones 3 and 4. The *z* coordinate was the height of the trajectory above the ground. Microphones 1, 3 and 4 were 1.16 m above the ground. The filled grey circles represent the position of the microphones that would fall within the coordinates shown in the figure.

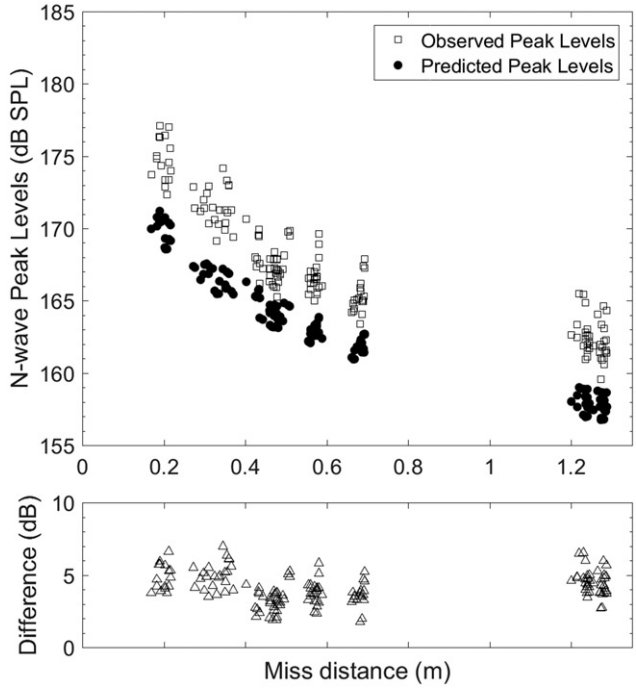

Figure 5. Top panel: The peak sound pressure levels predicted using Equation 1 for all shots (filled circles) and observed peak levels (squares). Black circles represent recordings from microphones 1 and 2. Bottom panel: The observed minus predicted differences as a function of the miss distance for microphones 1 and 2 (see text for details). There was no meaningful change in the prediction errors as a function of the distances assessed in this study.

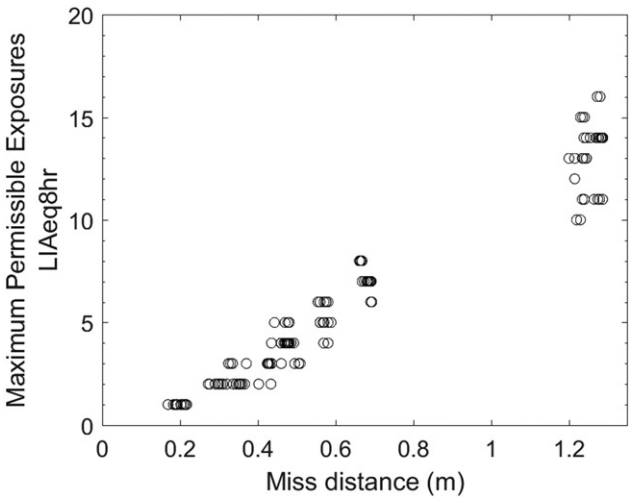

Figure 6. The maximum permissible exposures (MPE) for the A-weighted equivalent 8-h exposures as a function of miss distance. The MPEs for the AHAAH model were all less than 1 exposure.

unprotected exposure would be permitted via this metric at miss distances less than about 25 cm. The MPE value increased to between 10 and 16 unprotected exposures at a miss distance of approximately 1.2 m. The MPE values returned from unwarned ARUs were less than 1 at all miss distances evaluated in this study and would not be allowed. Although there were large differences in MPE values across risk metrics, the logarithms of the metrics were strongly related ($r = 0.90$; $p < 0.001$). A univariable regression model predicting the logarithm of MPE values from unwarned ARUs based on log MPE values from $L_{IAeq8hr}$ indicated that the unwarned ARU

$$\log(MPE_{ARU}) = 0.31\left(\log(MPE_{LIAeq8hr})\right) - 0.62. \quad (12)$$

Inferential analyses yielded a model of MPE as follows:

$$MPE_{LIAeq8hr} = -28.01 + 11.79b + 0.08779v - (8 \times 10^{-5})v^2 + 155.7l. \quad (13)$$

indicating that MPE estimated using the $L_{IAeq8hr}$ metric increased with miss distance (see also Figure 6), departed from linearity at the greatest velocities, and increased with bullet length. The model was highly significant (χ^2_4=6699; $p < 0.0001$) and individual model coefficients were significant at or below the $p > 0.002$ level. Together, these predictors led to estimates within one MPE (range −0.43 to 0.57 MPE).

The inferential model of MPE estimated using the unwarned AHAAH metric consisted of significant coefficients only for miss distance and velocity (model χ^2_2=772; $p < 0.0001$), but this difference could be associated with the lower MPE variance associated with this metric. The regression equation is not presented because, as noted above, all MPE using the unwarned AHAAH metric were less than 1.0 and therefore the equation provides no practical guidance at the distances evaluated in the present study.

Discussion

The purpose of this study was to evaluate the potential auditory hazard associated with unprotected exposure to ballistic N-waves generated by a selection of 0.50 Beowulf® ammunition models. The results of this study indicated that these exposures present a substantial risk of noise-induced hearing loss. Estimated MPE based on the $L_{IAeq8hr}$ metric increased as a function of miss distance, departed from a linear increase with increased bullet velocity, and increased with bullet length. The MPE estimates based on the AHAAH metric were related only to miss distance and bullet velocity.

Multiple prior studies have demonstrated that the equation relating the acoustic characteristics of the N-wave to fundamental projectile characteristics (Whitham, 1974) underestimates observed peak levels (Stoughton, 1997). The Whitham equation was developed for far-field applications (e.g. at miss distances of 1000 bullet diameters or 12.7 metres for a 0.50 calibre bullet (Whitham, 1974)). Measurements presented in this study were taken at miss distances around 20–100 bullet diameters from the trajectory, and if the deviation were solely associated with the application of a far-field relation to near-field signals, the deviation (Figure 5, lower panel) from predictions would be expected to decline with increased miss distance. It is possible that this reduction was not observable across the short range of miss distances used in this study.

Studies of the ballistic N-wave have focussed primarily on utilising the precursor to the muzzle blast in the context of locating the position of an opponent who is firing upon an observer. For example, technologies used in urban environments aid law enforcement personnel locating a shooting event in a complex acoustic environment due to the multitude of reflections (Hewett, 2010; Korman and Sarkady, 2013). The auditory risks of ballistic N-wave exposure involving the 0.50 Beowulf® rifle have not been reported previously. It is important to recognise that no damage-risk criterion has been developed or tested using human exposures to ballistic N-waves, perhaps owing to the combined auditory and non-auditory hazards of conducting such a study. Fedele (2018) also applied these damage-risk criteria to N-waves and found a similar difference in the permissiveness of the damage-risk criteria used in this study and that one or two exposures to ballistic N-wave produced by 5.56 mm and 7.62 mm ammunition would be permitted using the AHAAH model.

The current study provides a method and illustrative results suggesting that hazardous noise is produced by bullets fired from a 0.50 Beowulf® rifle at a down range distance of 6.4 metres at miss distances of up to 1.2 metres. The generalisability of these results to other distances (either down range or miss distances), bullet dimensions, or velocities remains unknown. The differences between observed peak levels and those predicted by Equation 1 could be amenable to a simple correction, and additional research covering a broader range of projectile dimensions and velocities would be required to develop that correction factor. However, an improved prediction of a peak sound pressure level would not be sufficient to provide estimates of auditory risk, which require more information than peak levels provide. Direct measurements of the waveforms with instruments capable of handling these signals will be necessary until such predictions are available.

Conclusion

The current study describes the auditory risk of unprotected exposure to ballistic N-waves produced by a 0.50 calibre rifle at relatively close distance (6.4 m) and distances from the trajectory at or below 1.3 m. Both damage-risk metrics included in MIL-STD-1474E (2015) returned MPE values suggesting that these sounds pose a risk to the ears of an unprotected listener.

Acknowledgements

We wish to acknowledge the contributions of First Sergeant Matthew Burkhardt with the Indiana State Police, Versailles District for the use of the firearm used in this study and for arranging to conduct this study at an outdoor firing range.

Disclaimer and Declaration of interest

The findings and conclusions in this report are those of the authors and do not represent any official policy of the Centers for Disease Control and Prevention or the National Institute for Occupational Safety and Health. Mention of company names and products does not constitute endorsement by the CDC or NIOSH.

The authors report no declarations of interest.

References

DuMond, J. W. M., E. R. Cohen, W. K. H. Panofsky, and E. Deeds. 1946. "Wave Forms and Laws of Propagation and Dissipation of Ballistic Shock Waves." *Journal of the Acoustical Society of America* 18 (1):97–118. doi:10.1121/1.1916347.

Fedele, P. D., D. B. Grasing, and C. C. Stachowiak 2018. *Auditory hazards due to small arms use in squad combat formations. Report ARL-TR-8334.* Aberdeen Proving Ground, MD: U.S. Army Research Laboratory. [Abstract Unclassified; Report: For Official Use Only.]

Flamme, G.A., A. Wong, K. Leibe, and J. Lynd 2009. Estimates of auditory risk from outdoor impulse noise II: Civilian firearms. *Noise and Health* 11:231–242. doi: 10.4103/1463-1741.56217.

Hewett, D. P. 2010. *Sound Propagation in an Urban Environment*. Ph.D. Dissertation, St. Catherine's College, Oxford University.

Huber, P. J. 1967. The behavior of maximum likelihood estimates under non-standard conditions. In Vol.1 *of proceedings of the fifth berkeley symposium on mathematical statistics and probability.*, 221–233. Berkeley: University of California Press.

Korman M. S., and A. A. Sarkady. 2013. Ballistic shock wave localization estimation of shooter psoition and velocity using difference of time of arrival DTOA algorithm in orthogonally arranged discrete acoustic arrays. *Proceedings of Meetings of Acoustics* 19, 045070. doi: 10.1121/4799802.

Landau, L. D. 1945. "On Shock Waves at Large Distances from the Place of Their Origin." *Journal of Physics USSR* 9:496–504.

Settles, G. S. 2001. *Schlieren and Shadowgraph Techniques: Visualizing Phenomena in Transparent Media*. Berlin: Springer-Verlag.

Stoughton, R. 1997. "Measurements of Small-Caliber Ballistic Shock Waves in Air." *Journal of the Acoustical Society of America* 102 (2):781–787. doi: 10.1121/1.419904.

United States Department of Defense 2015. *MIL-STD-1474E Design criteria standard: Noise limits*. Washington DC: U.S. Department of Defense.

Varnier, J., and F. Sourgen. 2014. "The Ballistic Wave, from Rifle Bullet to Apollo Command Module." *Acoustics in Practice* 2 (2):43–51. https://hal.archives-ouvertes.fr/hal-01103309/document

Whitham, G. B. 1974. *Linear and Nonlinear Waves*. New York: John Wiley & Sons.